poor prognosis.[6] Therefore, to date, it remains unclear whether there is down-regulation of maspin during ductal carcinoma progression. To clarify our hypothesis that maspin expression may be up-regulated during ductal carcinoma progression, we investigated the expression of maspin in a large number of DCIS and IDC with a predominant intraductal component as well as atypical ductal hyperplasia and usual ductal hyperplasia.

Materials and methods

CASES STUDIED

The cases examined in this study were retrieved from the surgical pathology files of the Department of Pathology, Kagoshima University, Japan. The 145 cases of DCIS were categorized into high, intermediate and low grades according to the Van Nuys classification.[7] No cases had axillary lymph node metastases. The 92 cases of IDC with a predominant intraductal component, in which the amount of invasive component was less than one-quarter of the intraductal component,[8] consisted of 18 cases of pT1mic (microinvasion), 47 cases of pT1a (the greatest dimension of invasion was more than 1 mm but not more than 5 mm) and 27 cases of pT1b (the greatest dimension of invasion was more than 5 mm but not more than 10 mm) according to the criteria of the TNM classification.[9] Three cases showed axillary lymph node metastases. In cases in which it was difficult to determine the presence of invasion, differential diagnoses between DCIS and IDC with a predominant intraductal component were aided by immunohistochemical detection of type IV collagen as described previously,[10] and α-smooth muscle actin. All cases of DCIS and IDC with a predominant intraductal component were only diagnosed in almost completely sectioned specimens. Atypical ductal hyperplasia (27 cases) and usual ductal hyperplasia (94 cases) were selected according to the criteria of Page and Rogers.[11] Atypical ductal hyperplasia was defined as a lesion showing some of the features of DCIS but falling short of a fully developed picture, and with an overall dimension of the lesion of <3 mm.

IMMUNOHISTOCHEMISTRY

Specimens were fixed in 10% neutrally buffered formalin, and embedded in paraffin. After blocking the endogenous peroxidase activity, deparaffinized sections (3 μm thick) were pretreated in 10 mM citrate buffer (pH 6) by microwaving (500 W, full power) for 15 min. After cooling for 60 min, the sections were incubated with primary antibodies overnight at 4°C in a moist chamber. The primary antibodies used were monoclonal anti-human maspin antibody directed against the N-terminal region of the human maspin molecule (clone, EAW24; Novocastra, Newcastle-upon-Tyne, UK) diluted 1 : 200, and monoclonal anti-oestrogen receptor (ER) antibody (clone, 1D5; Immunotech, Marseille, France) diluted 1 : 1. The sections were incubated with biotinylated goat anti-mouse immunoglobulin (diluted 1 : 150; Vector Labs, Burlingame, CA, USA) for 15 min, followed by horseradish peroxidase-conjugated streptavidin complex for 10 min (diluted 1 : 100; Zymed, San Francisco, CA, USA). To visualize the immunoreactivity, diaminobenzidine tetrachloride (1 mg/ml) containing 0.1% hydrogen peroxidase (30% w/v) was used. Negative controls for maspin antibody were performed using non-immune serum instead of the primary antibody or axillary lymph node sections. Nude mice tumours originating from human prostate cancer PC-3 cells, which showed high levels of maspin mRNA expression, were used as positive controls.[12,13] Myoepithelial cells in the same section, which are known to express maspin protein,[1] served as internal positive controls.

HISTOLOGICAL SCORING

The cells were considered positive for maspin expression only when distinct cytoplasmic staining was identified. To count the number of positive cells, a 10 × 10 square grid in the eyepiece was used. The sections were scanned at low- and high-power magnifications covering all fields. At least three areas with the highest degree of positive cells were selected, and typically 400–500 tumour cells in each field were counted irrespective of immunoreactive status. Thereafter, positive cells were counted and the percentage of positive cells was determined. Tumours with >10% of positive cells were considered positive for the expression of maspin. Distinct nuclear staining was considered as positive cells for ER, and cases with >10% of positive cells were interpreted as ER+.[14]

STATISTICAL ANALYSIS

All statistical analyses were performed using the Dr. SPSS software package (Release 8.0J; SPSS Japan Inc., Tokyo, Japan). χ^2 analysis was used to calculate the significance of difference. The cut-off for significance was taken as $P = 0.05$.

ETHICAL APPROVAL

This study, which involved the use of archival tissues from human subjects, was approved by the ethical committee at the Faculty of Medicine, Kagoshima University.

Results

In normal breast tissue, both the cytoplasm and nuclei of myoepithelial cells were vividly stained throughout (Figure 1). No positive staining was observed in the epithelial cells. Only one case of usual ductal hyperplasia showed positive staining in the epithelial cells (Figure 2). No positive staining was observed in the epithelial cells in any of the atypical ductal hyperplasia cases (Figure 3). The expression of maspin in the carcinoma cells was found in 14 (9.6%) of the 145 DCIS cases. A representative staining pattern is shown in Figure 4. The staining pattern within specimens was heterogeneous, with both positively and negatively stained cells evident in the tumour foci. The number of samples and the percentages of positive cells were as follows: <10% positive cells in two samples; 10–50% positive cells in nine samples; >50% positive cells in five samples. Some cells also exhibited nuclear staining accompanied by cytoplasmic staining. The expression of maspin significantly correlated with larger tumour size ($P = 0.013$), higher histological grade ($P = 0.015$) and positive-comedo necrosis ($P = 0.000005$) (Table 1). No significant relationship was observed between the expression of maspin and ER ($P = 0.108$). The expression of maspin in carcinoma cells was found in 17 of the 92 IDC with a predominant intraductal component

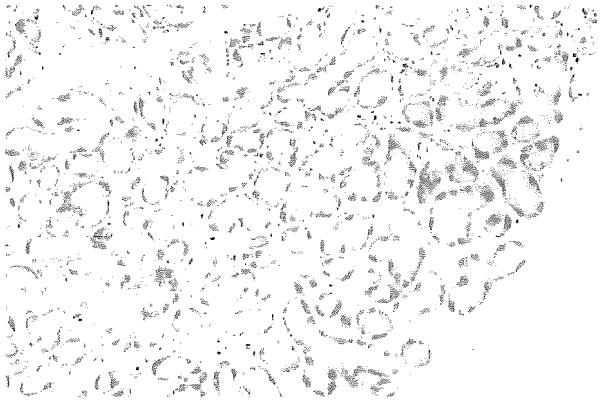

Figure 1. Normal breast tissue showing strong immunostaining for maspin in the cytoplasm and nuclei of myoepithelial cells. Epithelial cells are negatively stained.

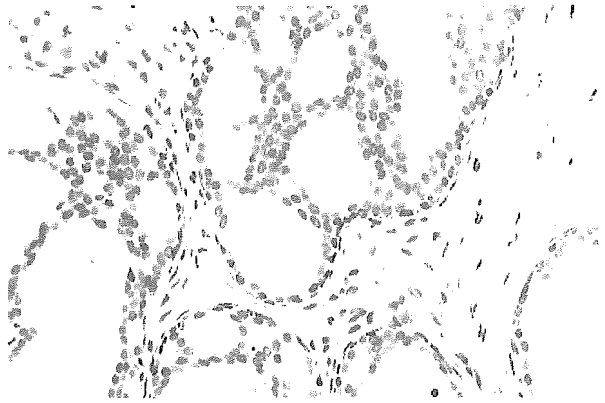

Figure 3. Atypical ductal hyperplasia showing strong immunoreactivity with maspin in the cytoplasm and nuclei of myoepithelial cells. Epithelial cells are negatively stained.

Figure 2. Usual ductal hyperplasia showing moderate immunoreactivity with maspin in the cytoplasm and nuclei of both epithelial and myoepithelial cells.

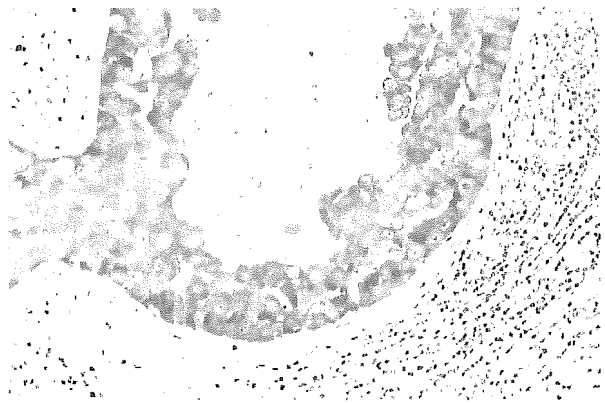

Figure 4. Typical example of ductal carcinoma in situ with comedo necrosis. Carcinoma cells are strongly immunostained for maspin.

Table 1. Association between maspin expression in ductal carcinoma in situ and clinicopathological parameters

	Maspin expression		
	Positive (9.6%) (14 tumours)	Negative (90.4%) (131 tumours)	*P*-value
Tumour size			
≤20 mm	2	63	0.013
>20 mm	12	68	
Oestrogen receptor			
Positive	7	92	0.108
Negative	7	39	
Histological grade			
Low	0	45	0.015
Intermediate	9	66	
High	5	20	
Comedo necrosis			
Present	14	51	0.000005
Absent	0	80	

Table 2. Association between maspin expression in invasive ductal carcinoma with a predominant intraductal component and clinicopathological parameters

	Maspin expression		
	Positive (18%) (17 tumours)	Negative (82%) (75 tumours)	*P*-value
Tumour size			
≤20 mm	5	42	0.042
>20 mm	12	33	
Histological grade of non-invasive ductal component			
Low	1	21	0.0003
Intermediate	4	38	
High	12	16	
Comedo necrosis			
Present	12	26	0.0074
Absent	5	49	

cases (18.5%). The positive rates of pT1mic, pT1a and pT1b were 11.2% (two of 18), 17% (eight of 47) and 25.9% (seven of 27), respectively. The expression of maspin significantly correlated with larger tumour size ($P = 0.042$), higher histological grade ($P = 0.0003$) and the presence of comedo necrosis ($P = 0.0074$) (Table 2).

Discussion

The tumour suppressor gene *maspin* is a unique member of the serpin (serine protease inhibitor) superfamily.[1] It has been shown to have tumour suppressive activity attributable to the inhibition of breast cancer cell motility, invasion and metastasis.[1,3] It appears that maspin expression is frequently lost in advanced breast cancer.[1] Maass *et al.* reported that down-regulation of the *maspin* gene in breast carcinoma was associated with a higher risk of distant metastasis using reverse transcription-polymerase chain reaction (RT-PCR).[15] Since human mammary myoepithelial cells surrounding normal duct and non-invasive ductal components express the maspin protein,[16] it could be difficult to evaluate 'maspin expression' in carcinoma cells by means of RT-PCR. In turn, it has been reported that a maspin transcript in bone marrow was detected in 32% of early-stage breast cancer patients, and in 75% of patients with metastatic breast cancer by means of RT-PCR assay.[17] Therefore, to date, it remains unclear whether there is down-regulation of maspin during ductal carcinoma progression. These discrepancies may be largely attributable to the lack of systematic immunohistochemical studies. Recently, Maass *et al.* reported that a significant stepwise decrease in maspin expression occurred in the sequence of DCIS–invasive cancer–lymph node metastasis. However, the number of DCIS was small ($n = 12$) and atypical ductal hyperplasia or IDC with a predominant intraductal component were not investigated in their study. Recently, we reported that the expression of maspin was observed in 27.4% of IDC and was correlated with an aggressive phenotype.[6] In the same study, we also investigated 58 cases of DCIS with a 20% cut-off and no positive cases were detected.[6]

In this study, we used a 10% cut-off instead of a 20% cut-off because of lower percentages of positive cells in DCIS compared with invasive ductal carcinoma, and demonstrated a stepwise increase in the frequency of maspin expression from DCIS to IDC with a predominant intraductal component (approximately two-fold). In addition, differences in frequency between DCIS and IDC are approximately three-fold according to our previous study.[6] The precise reason for the discrepancies between our and Maass's studies is unclear, but some factors, such as differences in the types of antibodies used, the methods of immunohistochemistry, criteria for positive staining and sample number,

may be in part responsible. We have revealed for the first time that the expression of maspin detected by immunohistochemistry is significantly correlated with an aggressive phenotype characterized by higher histological grade, larger tumour size and the presence of comedo-necrosis in a large number of DCIS cases. The expression of maspin in the epithelial cells of atypical ductal hyperplasia and usual ductal hyperplasia was very rare. Moreover, we have demonstrated a stepwise increase in the frequencies of maspin expression in the carcinoma cells during ductal carcinoma progression. Taken together, our results suggest that the expression of maspin in epithelial cells could be up-regulated during ductal carcinoma progression, and that it could be relevant to the acquisition of an aggressive phenotype.

The precise mechanism of the aberrant expression of maspin in carcinoma cells remains unclear, but we can consider three possible explanations. One is the mutation of the *maspin* gene causing loss of normal function of the maspin protein, the second is a high intracellular concentration of maspin resulting in auto-inhibition of its activity by non-covalent polymerization.[18] The third is that myoepithelial cell differentiation in carcinoma cells could contribute to the more aggressive phenotype[19] if the expression of maspin is a true marker of myoepithelial cell differentiation. Additionally, the finding of maspin expression in a high percentage of high-grade pancreatic cancers[20] and ovarian cancer[21] as well as our previous report suggesting the role of maspin expression in breast cancer as a poor prognostic factor[6] challenge the concept of the tumour-suppressing abilities of maspin. Further investigation to clarify the precise mechanisms of the aberrant expression of maspin in DCIS with an aggressive phenotype are needed.

Acknowledgements

The authors are grateful to Mr M. Soda and Mr T. Kodama for their assistance with the immunohistochemical analysis. This work was supported in part by a grant (13670181) from the Ministry of Education, Science, Sports and Culture, Japan and the Kodama Memorial Fund for Medical Research.

References

1. Zou Z, Anisowicz A, Hendrix MJ *et al.* Maspin, a serpin with tumor-suppressing activity in human mammary epithelial cells. *Science* 1994; **263**; 526–529.
2. Sheng S, Pemberton P, Sagar R. Production, purification and characterization of recombinant maspin protein. *J. Biol. Chem.* 1994; **269**; 30988–30993.
3. Sheng S, Carey J, Seftor EA *et al.* Maspin acts at the cell membrane to inhibit invasion and motility of mammary and prostatic cancer cells. *Proc. Natl Acad. Sci. USA* 1996; **93**; 11669–11674.
4. Sheng S, Truong B, Fredrickson D *et al.* Tissue-type plasminogen activator is a target of the tumor suppressor gene maspin. *Proc. Natl Acad. Sci. USA* 1998; **95**; 499–504.
5. Maass N, Teffner M, Rosel F *et al.* Decline in the expression of the serine proteinase inhibitor maspin is associated with tumor progression in ductal carcinoma of the breast. *J. Pathol.* 2001; **195**; 321–326.
6. Umekita Y, Ohi Y, Sagara Y *et al.* Expression of maspin predicts poor prognosis in breast-cancer patients. *Int. J. Cancer* 2002; **100**; 452–455.
7. Silverstein MJ, Poller DN, Waisman JR *et al.* Prognostic classification of breast ductal carcinoma-in-situ. *Lancet* 1995; **345**; 1154–1157.
8. World Health Organization. *Histological typing of breast tumours*, 2nd edn. Geneva: WHO, 1981.
9. UICC International Union Against Cancer. Breast tumours. In Sobin LH, Wittekind C eds. *TNM classification of malignant tumours*, 5th edn. New York: Wiley-Liss, 1997; 123–130.
10. Umekita Y, Takasaki T, Yoshida H. Expression of p53 protein in benign epithelial hyperplasia, atypical ductal hyperplasia, non-invasive and invasive mammary carcinoma: an immunohistochemical study. *Virchows Arch.* 1994; **424**; 491–494.
11. Page DL, Rogers LW. Combined histologic and cytologic criteria for the diagnosis of mammary atypical ductal hyperplasia. *Hum. Pathol.* 1992; **23**; 1095–1097.
12. Umekita Y, Hiipakka RA, Liao S. Rat and human maspins: structures, metastatic suppressor activity and mutation in prostate cancer cells. *Cancer Lett.* 1997; **113**; 87–93.
13. Umekita Y, Hiipakka RA, Kokontis JM *et al.* Human prostate tumor growth in athymic mice: inhibition by androgens and stimulation by finasteride. *Proc. Natl Acad. Sci. USA* 1996; **93**; 11802–11807.
14. Hendricks JB, Wilkinson EJ. Comparison of two antibodies for evaluation of estrogen receptors in paraffin-embedded tumors. *Mod. Pathol.* 1993; **6**; 765–770.
15. Maass N, Hojo T, Rosel F *et al.* Down regulation of the tumor suppressor gene maspin in breast carcinoma is associated with a higher risk of distant metastasis. *Clin. Biochem.* 2001; **34**; 303–307.
16. Sternlichit MD, Kedeshian P, Shao ZM *et al.* The human myoepithelial cell is a natural tumor suppressor. *Clin. Cancer Res.* 1997; **3**; 1949–1958.
17. Ballestrero A, Coviello DA, Garuti A *et al.* Reverse-transcriptase polymerase chain reaction of the maspin gene in the detection of bone marrow breast carcinoma cell contamination. *Cancer* 2001; **92**; 2030–2035.
18. Liu T, Pemberton PA, Robertson AD. Three-state unfolding and self association of maspin, a tumor-suppressing serpin. *J. Biol. Chem.* 1999; **274**; 29628–29632.
19. Jones C, Nonni AV, Fuitord L *et al.* CGH analysis of ductal carcinoma of the breast with basaloid/myoepithelial cell differentiation. *Br. J. Cancer* 2001; **85**; 422–427.
20. Maass N, Hojo T, Ueding M *et al.* Expression of the tumor suppressor gene Maspin in human pancreatic cancers. *Clin. Cancer Res.* 2001; **7**; 812–817.
21. Sood AK, Fletcher MS, Gruman LM *et al.* The paradoxical expression of maspin in ovarian carcinoma. *Clin. Cancer Res.* 2002; **8**; 2924–2932.

LY309887, antifolate via the folate receptor suppresses murine type II collagen-induced arthritis

R. Nagayoshi[1], M. Nakamura[2], K. Ijiri[3], H. Yoshida[4], S. Komiya[1], T. Matsuyama[2]

[1]Department of Orthopaedic Surgery, [2]Department of Immunology, [3]Department of Physiotherapy, and [4]First Department of Pathology, School of Medicine, Kagoshima University, Sakuragaoka, Kagoshima City, Japan.

Abstract

Objective

To examine the effect of LY309887, an inhibitor of glycinamide ribonucleotide formyltransferase in de novo *purine biosynthesis on murine type collagen-induced arthritis (CIA).*

Methods

CIA was induced by immunization with bovine type II collagen in adjuvant. The expression of folate receptors was examined in dissected synovial tissues and bone marrow cells from arthritic and non-arthritic mice by the semi-quantitative reverse transcription-polymerase chain reaction. LY309887 was administered to CIA mice after the onset of arthritis. Mice were monitored for arthritis index for 21 days. Levels of IgG_1 and IgG_{2a} antibodies against bovine type II collagen were measured in sera from CIA mice with or without LY309887 treatment by the enzyme-linked immunosorbent assay. Histologic analyse were also performed in synovial tissues from arthritic joints with or without LY309887 treatment.

Results

Levels of mRNA of folate receptor beta (FR-β) were elevated in arthritic joints from CIA mice, compared with those in nonarthritic joints. The expression of mRNA of FR-β was dominant in bone marrow cells of CIA mice. The administration of LY309887 suppressed the disease progression of CIA mice as defined by the lower arthritis index, and decreased production of serum IgG_1 and IgG_{2a} anti-type II collagen antibody, and the damage to cartilage or bone.

Conclusion

The administration of LY309887 was effective on CIA mice. It was suggested that LY309887 might be useful in the treatment of rheumatoid arthritis.

Key words

Antifolate, folate receptor, collagen type II, arthritis.

Ryusaku Nagayoshi, MD; Setsuro Komiya, MD, PhD; Motoyuki Nakamura, PhD; Takami Matsuyama, MD, PhD; Kosei Ijiri, MD, PhD; Hiroki Yoshida, MD, PhD.

This work was supported by grants from the Japanese Ministry of Culture, Education, and Science.

Please address correspondence and reprint requests to: Dr. T. Matsuyama, Department of Immunology, School of Medicine, Kagoshima University, 8-35-1 Sakuragaoka, Kagoshima City, Japan 890-8520. E-mail: matuyama@m.kufm.kagoshima-u.ac.jp.

Received on March 31, 2003; accepted in revised form on July 18, 2003.

Introduction

It has been known that oxidized folates such as folic acid are transported via folate receptors (FRs), while reduced folates such as 5-methyl tetrahydrofolates and methotrexate are transported via reduced folate carrier (RFC) (1-3). At present, three folate receptors alpha (FR-α), beta (FR-β), gamma (FR-γ) are functionally identified in humans (4). FR-γ may not be functional as the membrane protein because it has an incomplete glycosylphosphatidyl inositol anchor portion. These receptors are expressed at low or undetectable levels in normal tissues and levels of their expression were elevated in epithelial and hematopioetic tumors. Thus, it is considered that folate derivatives with a high affinity for these receptors may become efficient drugs or be useful as drug delivery agents for the treatment of tumors (5, 6).

In rheumatoid arthritis (RA), the dominant cell type in the joints is the macrophage. Several reports showed a correlation between the number of macrophages present in the joint and severe cartilage destruction (7). In fact, selective removal of synovial macrophages after the onset of experimental arthritis downregulated synovial inflammation (8, 9). Previously, we showed that the expression of FR-β was selectively elevated in synovial macrophages from RA (10). Likewise, Turk *et al.* showed that folic acid was transported via the FRs, probably FR-β on activated macrophages in arthritic joints of mycoplasma-induced arthritic rat (11). These findings suggested to us that drugs with a high affinity for FR-β may selectively downregulate synovial inflammation mediated by synovial macrophages.

Recently, several reports showed the effectiveness of folate derivatives with a high affinity for FR-α on tumors in experimental models (12, 13). Among these drugs, LY309887 is a potent inhibitor of glycinamide ribonucleotide formyltransferase (GARFT) involved in *de novo* purine biosynthesis and it has a high affinity for FR-α and a significant affinity for FR-β. Most recently, it was reported that a phase I trial using LY309887 in humans was successfully performed (14).

In this study, we examined the expression of FRs in arthritic joints because there are no information about the expression of FRs in experimental arthritic joints. Furthermore, the effect of LY309887 on murine type II collagen-induced arthritis (CIA) was examined by means of clinical scores, serum levels of anti-type II collagen antibody, and histological analysis.

Materials and methods

Induction of arthritis

Seven-week-old male DBA/1J mice were purchased from Charles River Japan (Yokohama, Japan). The mice were housed in filter-topped cages, and water and a low-folate diet (0.02 mg%) (Dyets, Bethlehem, PA) were provided *ad libitum*. This study was carried out after permission was received from the Committee of Animal Experimentation, Faculty of Medicine, Kagoshima University.

Bovine type II collagen (C II) was prepared according to the method of Miller and Rhodes (15). Briefly, C II was diluted with 0.1 M acetic acid to a concentration of 4 mg/ml and was emulsified in an equal volume of Freund's incomplete adjuvant (IFA; Difco, Detroit, MI) containing H37Ra *Mycobacterium tuberculosis* (Difco). At the age of 9 weeks, the mice fed for at least two weeks with a low-folate diet were immunized intradermally at the base of the tail with 100 μl emulsion (200 μg collagen).

LY309887, a gift from Lilly Research Laboratories, Indianapolis, IN, was diluted to 2.5 μg/ml or 7.5 μg/ml in phosphate-buffered saline (PBS).

Treatment and evaluation of arthritis

Mice were randomly assigned to 1 of 3 groups after the onset of arthritis: the low dose or high dose treatments with LY309887, or control. In LY309887 treatment, mice were treated with an injection of 200 μl solution containing 0.5 μg or 1.5 μg of LY309887 intraperitoneally on days 1, 3, 5, 7, and 9.

Mouse paws were scored for arthritis as previously described (16). Briefly, a 4-point scale was used, where 0 = normal, 1 = slight swelling and erythema, 2 = pronounced edema, and 3 = joint rigidi-

ty. The cumulative score of all 4 paws of each mouse was used as the "arthritis index" (maximum score of 12 per mouse) to represent the overall disease severity and progression in an animal.

Analysis of tissue samples

Arthritic and non-arthritic mice were killed on day 21 after the onset of arthritis. The arthritic joints and the clinically non-arthritic joints were dissected and used for the preparation of total RNA. Additionally, the bone marrow from arthritic and non-arthritic mice was dissected and used for preparation of total RNA.

Analysis was carried using the reverse transcription-polymerase chain reaction (RT-PCR). Total RNA was isolated using TRIzol LS reagent (Life Technologies, Gaithersburg, MD). The first strand cDNA kit (SuperScript Preamplication System; Life Technologies) was used to make cDNA from 5 μg of each RNA. Amplification of each cDNA was performed with a AccuPower PCR Premix kit (Bioneer, Seoul, Korea). Polymerase chain reaction (PCR) was performed according to a standard protocol. Primers used were as follows: FR-α CAGGAAGCACATAAGGACATT (upstream primer), TCAAACCACATCTGAATGCAG (downstream primer); FR-β CTCTTG CTTTTGGTCTACATG (upstream primer), GAAGTAGTACTCAAACGTGTG (downstream primer); RFC ACTAACGAGATCATTCCGATG (upstream primer), GATCTAGTTTCCTGGTTTCTG (downstream primer); GAPDH GGAGCCAAACGGGTCATCATCTC (upstream primer), ATGCCTGCTTCACCACCTTCTTG (downstream primer). The message for CD163 and IL-1β was amplified using the primers described elsewhere (17, 18). The amplified PCR products for FR-α, FR-β, IL-1β, RFC, CD163, and GAPDH were 430 basepairs (bp), 501 bp, 166 bp, 535 bp, and 151 bp, and 454 bp, respectively. In preliminary experiments, we examined linearity of PCR amplification of FR-α, FR-β, IL-1β, RFC, CD163, and GAPDH cDNA by increasing the number of PCR cycles from 18 to 35. Data indicated that PCR amplification of FR-β cDNA reached a plateu by 33 cycles. Therefore, we used 30 cycles to determine the relative abundance of FR-β mRNA. In the same way, we used 26 cycles, 28 cycles, 27 cycles, 26 cycles, and 21 cycles to determine those of FR-α, IL-1β, RFC, CD163, and GAPDH, respectively.

We then measured anti-collagen type II antibody (anti-C II). Individual serum samples were collected at the end of the experiment by retro-orbital puncture. They were divided into aliquots and stored at -20°C until they were used for the ELISA. Immunoplates (MaxiSorp; Nunc, Roskilde, Denmark) were coated overnight with 2 μg/ml of bovine type II collagen in PBS at 4°C. Non-specific binding was blocked with 10% fetal bovine serum (FBS) in PBS for 30 minutes at 37°C. Serum samples (diluted with 10% FBS-0.05% Tween 20 in PBS) were added and incubated for 2 hours at 37°C. Serum dilutions were chosen after preliminary assays and ranged from 1:400 to 1:40,000 for IgG_1 or IgG_{2a} anti-C II.

The plates were then incubated with biotinylated rabbit anti-mouse IgG_1 (Zymed, San Francisco, CA) or IgG_{2a} (Santa Cruz Biotechnology, Santa Cruz, CA) for 1.5 hrs at 37°C. Streptavidin-horseradish peroxidase (HRP; Zymed) was used as substrate, and the optical density (OD) at 405 nm was measured using a microplate reader (model 550; Bio-Rad, Hercules, CA). All incubations were carried out in a volume of 100 μl/well, and between steps the plates were washed 4 times with 200 μl 0.05% Tween 20 in PBS.

The relationship of the optical density measured in standard serum diluted serially and arbitrary units showed a good linear correlation in all determinations (data not shown). The concentrations of IgG_1 and IgG_{2a} anti-C II in the sera diluted 1:4000 are presented as relative values (arbitrary units) compared with the optical density of the standard sera. Each plate was incubated with a standard curve of positive serum used to define arbitrary units of total IgG_1 and IgG_{2a} anti-C II Abs.

Hematology and histopathology

White blood cell counts were performed on samples isolated by orbital vein puncture on day 21. Blood hemoglobin concentrations were measured using a diagnostic kit (Hemoglobin Test Wako, Wako Pure Chemical Company, Ltd., Osaka, Japan).

Arthritic hind paws from at least 4 mice from each group were collected at the end of the experiment, fixed with 10% buffered formalin, decalcified in 5% EDTA and then embedded in paraffin. Sagittal serial sections of whole hind paws (5 μm thickness) were cut and stained with hematoxylin and eosin for microscopic evaluation, which was performed in a blinded manner. To determine whether the treatment had an effect on the degree of joint inflammation, the ankle, the metatarsophalangeal and proximal and distal interphalangeal joints were examined for the presence or absence of synovitis, pannus formation, cartilage loss, bone erosions, and disruption of the joint architecture.

Statistical analysis

The non-parametric Mann-Whitney U test was used to test for differences in clinical parameters among mice across the experimental groups. $P \leq 0.05$ was accepted as significant. Data were analyzed using Stat-View 4.5 statistical software for Windows (SAS Institute, Cary, NC).

Results

Elevated levels of mRNA of FR-β in arthritic joints from CIA mice

We examined levels of mRNA of FR-α, FR-β, RFC, IL-1β and the macrophage-specific marker CD163 in the arthritic and non-arthritic joints of CIA mice by semi-quantitative RT-PCR analysis. As shown in Figure 1A, levels of mRNA of FR-β were elevated in arthritic joints compared to those in non-arthritic joints and paralleled those of IL-1β in both joints. In contrast the levels of mRNA of RFC and CD163 detected were similar between arthritic and non-arthritic joints. Levels of mRNA of FR-α were not detectable in either joints (data not shown). In human tissues, it was reported that the expression of mRNA of FR-β was observed in myeloid lineage cells of

the bone marrow (19, 20). To determine the expression of mRNA of FR-β in murine bone marrow cells, we examined levels of mRNA of FRs in the bone marrow of CIA mice. The expression of mRNA of FR-β and RFC but no expression of mRNA of FR-α were observed in the bone marrow of CIA mice (Fig. 1B).

Suppression of clinical symptoms in CIA mice by administration of LY309887

Mice were fed a low-folate diet during the experiments to obtain low-folate concentrations similar to those of humans. Previously, it was shown that low-folate serum concentrations enhanced the effects of LY309887 (21). In the pharmacokinetics of LY309887 in humans, it was reported that LY-309887 concentrations declined rapidly for 24 to 36 hours. Since the clearance of LY309887 in mice has been described to be close to that of humans, CIA mice were treated every other day. Preliminary experiments using our treatment protocol showed that the administration of 5 doses (1.5 μg/dose) every other day was safe and effective. CIA mice were treated with low (0.5 μg/dose) or high doses (1.5 μg/dose) of LY309887 and with PBS alone. As shown in Figure 2, on day 13 the high-dose treatment with LY309887 had significantly suppressed the development of clinical symptoms in CIA mice compared with the control group. In contrast, low-dose treatment with LY-309887 resulted in only a modest effect on the clinical symptoms of CIA mice. Concerning the white blood cell count, serum hemoglobin concentration, and body weight, no significant differences were found among these groups (data not shown). Additionally, no side effects (for example, diarrhea or hematochezia) were observed in either group during this experimental period.

Decreased production of IgG_1 and IgG_{2a} anti-C II in CIA mice following the administration of LY309887

We next examined antibody titers of IgG_1 and IgG_{2a} anti-C II in serum samples from treated and non-treated mice on day 21 after the onset of arthritis. As

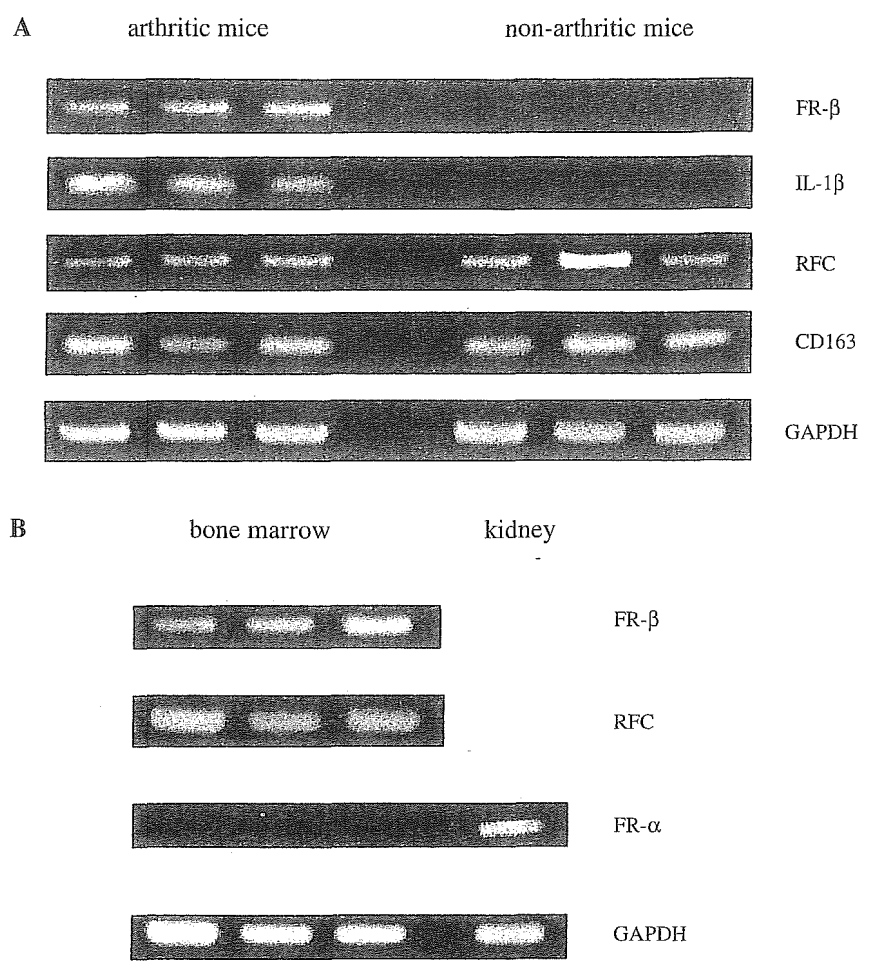

Fig. 1. (**A**) RT-PCR determination of selective FR-β mRNA expression in the joints of CIA mice. Total RNA was isolated from arthritic and non-arthritic joints of CIA mice and subjected to RT-PCR analysis for FR-β, IL-1β, RFC, CD163 and GAPDH. mRNA was collected from the dissected joints of 2 arthritic and 2 non-arthritic mice. (**B**) RT-PCR determination of selective FR-β mRNA expression in bone marrow cells of arthritic and non-arthritic mice. Total RNA was isolated from bone marrow cells of arthritic mice and subjected to RT-PCR analysis for FR-β, RFC, FR-α and GAPDH. Additionally, total RNA was isolated from the kidney of CIA mice and subjected to RT-PCR analysis for FR-α and GAPDH. Each mRNA was collected from bone marrow cells obtained from 2 arthritic mice.

shown in Figure 3, antibody titers of both IgG_1 and IgG_{2a} anti-C II in mice treated with high doses of LY309887 were lower than those in mice treated with PBS.

Reduction in CIA histopathology associated with administration of LY309887

Histologic analyses were performed in the hind limbs of mice treated with PBS or LY309887 on day 21 after the onset of arthritis. For a direct comparison between control and LY309887-treated mice, we selected animals whose arthritis index equaled the average arthritis index of their respective groups. The interphalangeal joints of a representative control mouse showed all the signs of severe inflammatory arthritis, including synovitis with massive infiltration of polymorphonuclear and mononuclear cells, pannus formation, cartilage erosion with loss of chondrocytes, and lateral bone resorption. The interphalangeal joints of a representative LY309887-treated mouse showed only mild synovitis and less damage to cartilage and bone (Fig. 4).

Discussion

In this study it was shown that levels of FR-β mRNA were elevated in arthritic joints of hind limbs compared to those in non-arthritic joints, whereas the levels of mRNA of CD163, macrophage-

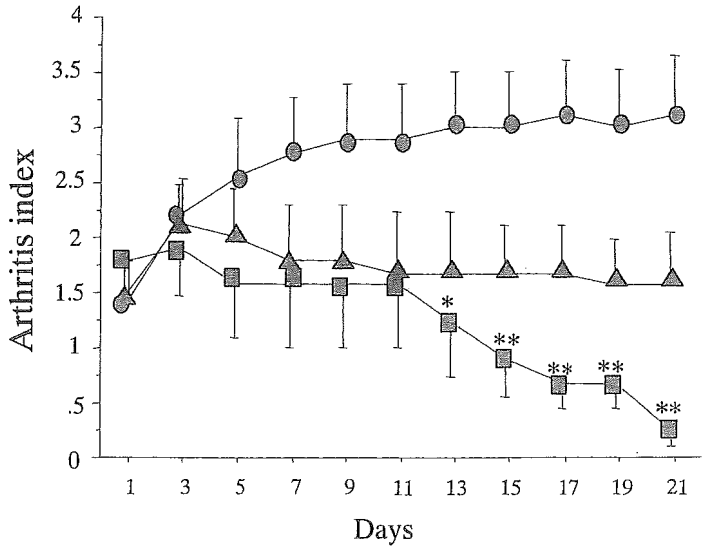

Fig. 2. Suppression of CIA by the administration of LY309887. After the onset of arthritis, mice were treated with intraperitoneal injections of 200 µl solutions containing 0.5 µg or 1.5 µg LY309887 on days 1, 3, 5, 7, and 9. Control mice were treated with PBS alone. ◉ control, ▲ LY309887, 0.5 µg/dose, ▣ LY309887, 1.5 µg/dose. Bars show the mean and SEM.
* $P < 0.03$ versus the control group. ** $P < 0.01$ versus the control group. P values were determined by the Mann-Whitney U test. Data are representative of two separate experiments with at least 9 mice per group.

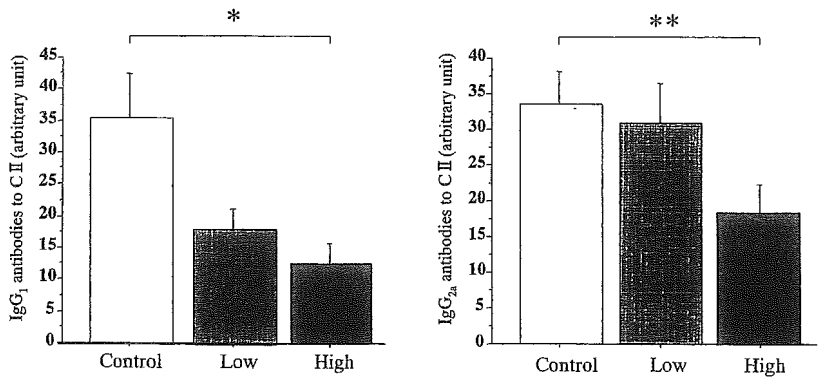

Fig. 3. Decreased production of IgG_1 and IgG_{2a} anti-C II in CIA mice by the administration of LY309887. Levels of IgG_1 (**A**) and IgG_{2a} (**B**) anti-C II were measured in sera from mice treated with PBS alone (controls, open bars), low dose LY309887 (gray bars) and high dose LY309887 (solid bars). After the onset of arthritis, mice were treated with 200 µl injections containing 0.5 µg or 1.5 µg of LY309887 intraperitoneally on days 1, 3, 5, 7, and 9. Control mice were treated with PBS alone. Bars show the mean and SEM. * $P < 0.01$ versus control group. ** $P < 0.02$ versus the control group. P values were determined by the Mann-Whitney U test.
Data are representative of two separate experiments with at least 9 mice per group.

specific marker detected were similar between these joints. In preliminary experiments involving immunohistochemical analysis of synovium from normal donors and RA patients for anti-FR-β specific antibody, the expression of FR-β protein was observed in synovial-infiltrated macrophages but not in resident synovial macrophage-like cells (synovial A cells). In contrast, similar expression of CD163 protein was observed in both macrophage subsets. Thus, the present findings support the notion that elevated levels of FR-β mRNA seen in the arthritic joints of CIA mice may be attributed to the increased percentage of synovial infiltrated macrophages.

In bone marrow cells of arthritic and non-arthritic mice, the expression of FR-β and RFC mRNA was observed, but not FR-α mRNA. These FR-β expressed cells are assumed to be monomyeloid lineage cells from previous findings in human bone marrow cells (19, 20).

Mouse CIA is mediated by synergistic T cells and humoral immune responses specific for type II collagen (22, 23). Additionally, there is accumulating evidence that macrophages and myeloid cells contribute to the severity and chronicity of synovial inflammation and cartilage destruction during experimental arthritis (8, 9).

The antiproliferation activity of antifolates depends on their ability to interact with intracellular folate-requiring enzyme targets, on their cellular transport properties and their degree of polyglutamation (13). LY309887 is thought to utilize RFC for uptake at high micromolar concentrations, and FRs at low serum concentrations (24). LY309887 has a high affinity for FR-α, and a 10-fold less affinity for FR-β and its polyglutamated form was shown intracellularly (12). It has been reported that LY-309887 is active in a broad spectrum of murine and human xenograft tumors and a phase I trial in humans has already been performed (12, 14). The intraperitoneal administration of LY309887 at 1.5 µg per dose every other day for a total of 5 doses was effective in CIA mice, as indicated by the clinical scores and histopathology of arthritic joints, and was well tolerated as reflected in the white blood cell count, serum hemoglobin and body weight. Thus, it is conceivable that LY309887 may act on proliferating monomyeloid lineage cells in bone marrow cells via FR-β. In fact, bone marrow suppression was reported as a side effect of LY309887 in murine tumor models (25). However, in this study we did not find a significant difference in the white blood cell count between treated and untreated mice. Therefore, it seems that LY309887 does not act simply as an antiproliferative agent.

In contrast to myeloid lineage cells in bone marrow, most macrophages in synovitis are believed to be non-proliferating (26). Accordingly, the action of LY309887 on synovial macrophages must be different from the anti-proliferation effect in bone marrow cells. Sev-

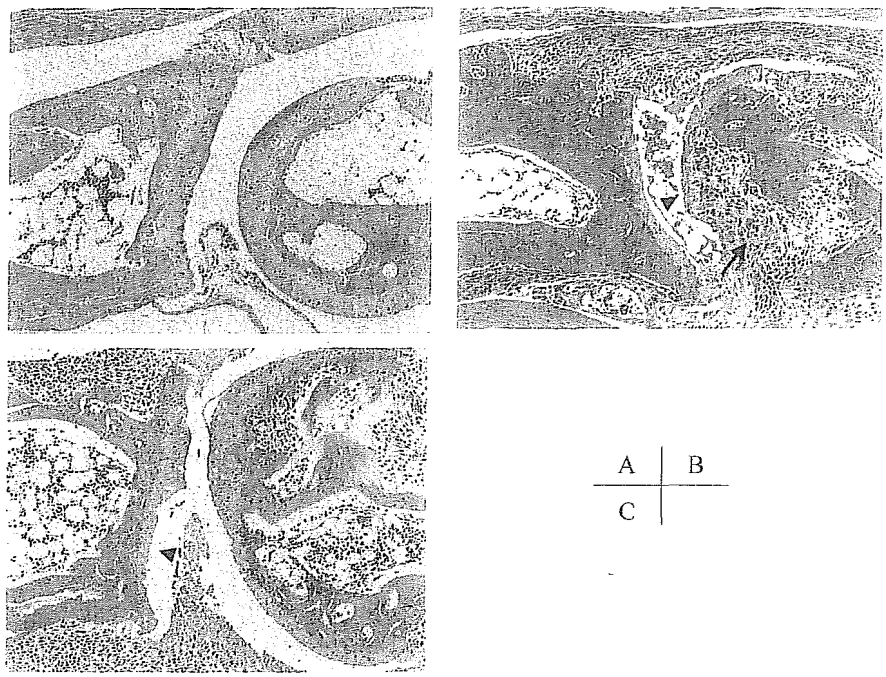

Fig. 4. Histopathology of collagen-induced arthritis (CIA) in PBS and LY309887 treated mice. For a direct comparison between control and LY309887 treated mice, we selected animals whose arthritis index equaled the average arthritis index of their respective group. All specimens were collected on day 21 after the onset of disease. (**A**) Normal interphalangeal (IP) joint. (**B**) Affected IP joint of a control mouse with an arthritic index of 2, showing severe synovitis with synovial hyperplasia and pannus formation (**arrow**), massive infiltration of polymorphonuclear and mononuclear cells, severe cartilage erosion (**arrowhead**) with loss of chondrocytes resulting in a pitted appearance of the surface, and lateral bone erosion. (**C**) Affected IP joints (as defined by footpad swelling) in LY309887-treated mice with an arthritic index of 2, displaying mild synovitis and less damage to the cartilage or bone (**arrowhead**). (Original magnification x100.)

eral lines of evidence clearly suggest that antifolates do not act simply as antiproliferative agents for the cells responsible for the joint inflammation in RA and the mechanism of action of low dose anti-folates might be more anti-inflammatory than antiproliferative (27). It has been suggested that LY309887 might inhibit aminoimidazolecarboximide ribonucleotide formyltransferase (AICARFT) activity, in addition to GARFT as a major target (12). In this regard, Cronstein *et al.* reported that MTX downregulates the inflammation of arthritis by the release of adenosine, strong anti-inflammatory metabolite via the inhibition of AICARFT (12, 13, 28). Thus, the effect of LY309887 on CIA mice may be due to the release of adenosine in arthritic joints. Furthermore, the effect of LY309887 might be attributed to the inhibition of mRNA and protein synthesis, which are elevated in inflammatory cells. Consequently, LY309887 may inhibit the production of inflammatory mediators such as proinflammatory cytokines, chemokines and metalloproteinases.

LY309887 suppressed the production of IgG_1 and IgG_{2a} anti-C II. It is well known that CIA is a Th1 cell-mediated disease and that IgG_{2a} anti-C II plays a role in the pathogenesis of arthritis by activating complement levels (29). IL-12 from activated macrophages promotes the development of Th1 cells that help IgG_{2a} production. Thus, suppression of the proliferation or activity of macrophages by LY309887 may cause the decreased production of IgG_{2a} anti-C II. At present, the significance of a marked reduction in IgG_1 anti-C II in the pathogenesis of CIA remains unknown. It was shown that myeloid lineage mast cells promote the development of Th2 cells by producing IL-4 and as a consequence promoting IgG_1 production (30). One possible explanation for the reduced production of IgG_1 anti-C II by LY309887 treatment is that LY309887 might also suppress the proliferation or activity of myeloid lineage mast cells.

The administration of LY309887 after the onset of arthritis prevented to a large extent the damage to cartilage and bone in arthritis, suggesting the possibility that this drug or reagents with a high affinity for FR-β might serve as disease-modifying drugs against RA. However, the use of folate during antifolate therapy must be considered on the basis of folate receptor competition in addition to competition with antifolate as a substrate for dihydrofolate reductase.

In conclusion, our findings support the hypothesis that LY309887 may be applicable to the treatment of RA by an alteration of the dosage protocol. In particular, the administration of LY309887 might be useful as a therapeutic agent in MTX-resistant RA patients, in that it acts on a different enzyme target from that of MTX.

Acknowledgments

The authors are would like to express their thanks to T. Kodama for his helpful technical assistance.

References

1. SADASIVAN E, ROTHENBERG SP: The complete amino acid sequence of a human folate binding protein from KB cells determined the cDNA. *J Biol Chem* 1989; 264: 5806-11.
2. RATNAM M, MARQUARDT H, DUHRING JL, FREISHEIM JH: Homologous membrane folate binding proteins in human placenta: Cloning and sequence of a cDNA. *Biochemistry* 1989; 28: 8249-54.
3. WONG SC, PROEFKE SA, BHUSHAN A, MATHERLY LH: Isolation of human cDNA that restore methotrexate sensitivity and reduced folate carrier activity in methotrexate transport-defective Chinese hamster ovary cells. *J Biol Chem* 1995; 270: 17468-75.
4. SHEN F, ROSS JF, WANG X, RATNAM M: Identification of a novel folate receptor, a truncated receptor, and receptor type beta in hematopoietic cells: cDNA cloning, expression, immunoreactivity, and tissue specificity. *Biochemistry* 1994; 33: 1209-15.
5. WANG S, LOW PS: Folate-mediated targeting of antineoplastic drugs, imaging agents, and nucleic acids to cancer cells. *J Control Release* 1998; 53: 39-48.
6. LEAMON CP, LOW PS: Folate-mediated targeting: from diagnostics to drug and gene delivery. *Drug Discov Today* 2001; 6: 44-51.
7. MULHERIN D, FITZGERALD O, BRESNIHAN B: Synovial tissue macrophage populations and articular damage in rheumatoid arthritis. *Arthritis Rheum* 1996; 39: 115-24.

8. VAN LENT PL, VAN DEN BERSSELAAR LA, VAN DEN HOEK AE, VAN DE LOO AA, VAN DEN BERG WB: Cationic immune complex arthritis in mice-a new model. Synergistic effect of complement and interleukin-1. *Am J Pathol* 1992; 140: 1451-61.
9. BLOM AB, VAN LENT PL, HOLTHUYSEN AE, VAN DEN BERG WB: Immune complexes, but not streptococcal cell walls or zymosan, cause chronic arthritis in mouse strains susceptible for collagen type II autoimmune arthritis. *Cytokine* 1999; 11: 1046-56.
10. NAKASHIMA-MATSUSHITA N, HOMMA T, YU S *et al.*: Selective expression of folate receptor β and its possible role in methotrexate transport in synovial macrophages from patients with rheumatoid arthritis. *Arthritis Rheum* 1999; 42: 1609-16.
11. TURK MJ, BREUR GJ, WIDMER WR *et al.*: Folate-targeted imaging of activated macrophages in rats with adjuvant-induced arthritis. *Arthritis Rheum* 2002; 46: 1947-55.
12. MENDELSOHN LG, SHIH C, SCHULTZ RM, WORZALLA JF: Biochemistry and pharmacology of glycinamide ribonucleotide formyltransferase inhibitors: LY309887 and lometrxol. *Invest New Drugs* 1996; 14: 287-94.
13. NEWELL DR: Clinical pharmacokinetics of antitumor antifolates. *Semin Oncol* 1999; 26: 74-81.
14. BUDMAN DR, JOHNSON R, BARILE B *et al.*: Phase I and pharmacokinetic study of LY309887: A specific inhibitor of purine biosynthesis. *Cancer Chemother Pharmacol* 2001; 47: 525-31.
15. MILLER EJ, RHODES RK: Preparation and characterization of the different types of collagen. *Methods Enzymol* 1982; 82: 33-65.
16. WILLIAMS RO, FELDMANN M, MAINI RN: Anti-tumor necrosis factor ameliorates joint disease in murine collagen-induced arthritis. *Proc Natl Acad USA* 1992; 89: 9784-8.
17. SHAER DJ, BORETTI FS, HONGEGGER A *et al.*: Molecular cloning and characterization of mouse CD163 homologue, a highly glucocorticoid-inducible member of the scavenger receptor cysteine-family. *Immunogenetics* 2001; 53: 170-7.
18. GABAY C, MARINOVA-MUTAFCHIEVA L, WILLIAMS RO *et al.*: Increased production of intracellular interleukin-1 receptor antagonist type I in the synovium of mice with collagen-induced arthritis. *Arthritis Rheum* 2001; 44: 451-62.
19. ROSS JF, WANG H, BEHM FG *et al.*: Folate receptor type beta is a neutrophilic lineage marker and is differentially expressed in myeloid leukemia. *Cancer* 1999; 85: 348-357.
20. REDDY JA, HANELINE LS, SROUR EF, ANTONY AC, CLAPP DW, LOW PS: Expression and functional characterization of the beta-isoform of the folate receptor on CD34 (+) cells. *Blood* 1999; 93: 3940-8.
21. ALATI T, WORZALLA JF, SHIH C *et al.*: Augmentation of the therapeutic activity of Lometrexol [(6-R)5,10-Dideazatetrahydrofolate] by oral folic acid. *Cancer Res* 1996; 56: 2331-5.
22. HOLMDAHL R, ANDERSSON M, GOLDSCHMIDT TJ, GUSTAFSSON K, JANSSON L, MO JA: Type II collagen autoimmunity in animals and provocations leading to arthritis. *Immunol Rev* 1990; 118: 193-232.
23. TERATO K, HASTY KA, REIFE RA, CREMER MA, KANG AH, STUART JM: Induction of arthritis with monoclonal antibodies to collagen. *J Immunol* 1992; 148: 2103-8.
24. WESTERHOF GR, SCHORNAGEL JH, KATHMANN I *et al.*: Carrier- and receptor-mediated transport of folate antagonists targeting folate-dependent enzymes: Correlates of molecular-structure and biological activity. *Mol Pharmacol* 1995; 48: 459-71.
25. CHEN VJ, BEWLEY JR, ANDIS SL *et al.*: Preclinical cellular pharmacology of LY23-1514 (MTA): A comparison with methotrexate, LY309887 and raltitrexed for their effects on intracellular folate and nucleoside triphosphate pools in CCRF-CEM cells. *Br J Cancer* 1998; 78: 27-34.
26. SCHASER K, KINNE RW, BEIL H, KLANDY B, STOSS H: Proliferation of T-cells, macrophages, neutrophilic granulocytes and fibroblast-like cells in the synovial membrane of patients with rheumatoid arthritis. *Verh Dtsch Ges Pathol* 1996; 80: 276-80.
27. CUTOLO M, STRAUB RH: Anti-inflammatory mechanisms of methotrexate in rheumatoid arthritis. *Ann Rheum Dis* 2001; 60: 729-35.
28. CRONSTEIN BN: Molecular therapeutics. *Arthritis Rheum* 1996; 39: 1951-60.
29. WATSON WC, TOWNES AS: Genetic susceptibility to murine collagen II autoimmune arthritis. Proposed relationship to the IgG2 autoantibody subclass response, complement C5, major histocompatibility complex (MHC) and non-MHC loci. *J Exp Med* 1985; 162: 1878-91.
30. FARRAR JD, ASNAGLI H, MURPHY K, MURPHY KM: T helper subset development: Roles of instruction, selection, and transcription. *J Clin Invest* 2002; 109: 431-5.

Toxicologic Pathology, 31:632–637, 2003

ISSN: 0192-6233 print / 1533-1601 online
DOI: 10.1080/01926230390241882

Rapid Emergence of Mammary Preneoplastic and Malignant Lesions in Human c-Ha-ras Proto-Oncogene Transgenic Rats: Possible Application for Screening of Chemopreventive Agents

YOICHIRO MATSUOKA,[1] KATSUMI FUKAMACHI,[1] TETSUYA HAMAGUCHI,[1] HIROYASU TORIYAMA-BABA,[1] HIROAKI KAWAGUCHI,[2] MASATO KUSUNOKI,[3] HIROKI YOSHIDA,[2] AND HIROYUKI TSUDA[1]

[1]*Experimental Pathology and Chemotherapy Division, National Cancer Center Research Institute, 5-1-1 Tsukiji, Chuo-ku, Tokyo 104-0045, Japan*
[2]*1st Department of Pathology, Faculty of Medicine, Kagoshima University, 8-35-1 Sakuragaoka, Kagoshima 890-8520, Japan, and*
[3]*2nd Department of Surgery, School of Medicine, Mie University, 2-174 Edobashi, Tsu, Mie 514-8507, Japan*

ABSTRACT

For comparison of mammary gland whole mounts with examination of 2 histologic sections of mammary gland, 56 Hras128 rats were intravenously injected with 50 mg/kg body weight of *N*-methyl-*N*-nitrosourea at 50 days of age and then sacrificed at days 5, 10, 15, 20, 25, and 56. Comparison of detection sensitivity between the whole mounts and histologic sections revealed no lesions apparent in whole mounts on day 10, although intraductal proliferation was clearly detected in histologic sections in 44% of treated rats. Proliferative lesions were first detected in whole mounts at a 44% incidence on day 15, while intraductal proliferations and atypical hyperplasias were apparent in the sections at 89% and 44% incidences, respectively. On day 20, atypical hyperplasias and small adenocarcinomas in histologic sections were found in almost all animals. In conclusion, examination of 2 histologic sections from mammary tissues was found to be practical for detection of small malignant lesions as early as 15 days after MNU injection, and suppressive effects of soy isoflavones were clearly evident within 20 days after carcinogen exposure. These results suggest that this model has practical utility for short-term screening of chemopreventive agents for mammary carcinogenesis.

Keywords. Breast cancer; chemoprevention; ductal hyperplasia; isoflavone; mammary gland; *N*-methyl-*N*-nitrosourea; ras; transgenic rat.

INTRODUCTION

Induction of mammary carcinogenesis by administration of either *N*-methyl-*N*-nitrosourea (MNU) or 7,12-dimethylbenz[*a*]anthracene (DMBA) to virgin female rats is widely used for experimental studies of mammary carcinogenesis (19, 22, 28, 32–34). Transgenic techniques have been used to create many animal models of human disease, and transgenic mice harboring the human c-Ha-ras proto-oncogene (1, 37), v-Ha-ras (29), or pim-1 (27) as well as *p53* knockout mice (10, 16) have been shown to be highly susceptible to tumor induction by certain carcinogens and therefore of possible use for rapid screening purposes (30). Recently, transgenic mouse lines harboring human oncogenes such as c-myc and TGFα or both, were reported to exhibit marked sensitivity to environmental liver carcinogens (35).

Despite frequent use in chemical carcinogenesis studies and also assays of carcinogenicity, only a few transgenic rat lines with high susceptibility to chemical carcinogenesis have been established (7, 12). We have generated one line carrying the human c-Ha-ras proto-oncogene (Hras128) that demonstrates high susceptibility regarding chemical induction of mammary, urinary bladder, and esophageal tumors (2, 3, 15). All of the females develop multiple mammary carcinomas within 8–12 weeks after administration of MNU or DMBA (2, 36). The period required for palpable tumor development is generally 28 and 40 days after MNU or DMBA administration, respectively, when nontransgenic female Sprague-Dawley (SD) rats are treated at 50–60 days of age (20, 31, 33). Stepwise progression from intraductal proliferation through ductal carcinoma in situ to invasive carcinomas has been reported with both carcinogens (20, 21). In terms of histogenesis, pathology, and sensitivity to hormones, the induced lesions closely resemble those in humans (21, 26).

The age-adjusted death rates from breast cancer are from 2- to 8-folds less in Asian countries than in the United States and Western Europe. This appears related to the 20–50 times greater consumption of soybean products (14, 18). In vivo and in vitro studies have indicated that genistein, one of the isoflavones in soybean, may be responsible for tumor suppressive effects (4, 5, 8, 24, 25).

In the present study, the process of carcinogenesis in a transgenic rat model was analyzed, concentrating attention on early lesion development. The abdominal-inguinal mammary glands (AIMG) were utilized in most of the analyses to determine sensitivity and practicability of our system, although rat mammary tissue is in fact composed of 6 pairs of the glands located from the upper thoracic to inguinal regions. Using this transgenic rat model in combination with a simple histology-based approach, tumor suppressive effects of soy isoflavones could be detected within a period as short as 20 days.

Address correspondence to: Hiroyuki Tsuda, Department of Molecular Toxicology, Nagoya City University Graduate School of Medical Sciences.

Abbreviations: MNU, *N*-methyl-*N*-nitrosourea; DMBA, 7,12-dimethylbenz(*a*)anthracene; PIL, proliferative intraductal lesions; AIMG, abdominal-inguinal mammary glands; SD, Sprague-Dawley; TEB, terminal endbud.

MATERIALS AND METHODS

Animals and Treatment

Hras128 and littermate nontransgenic female rats were bred under SPF conditions by CLEA Japan Co, Ltd, Tokyo. They were housed 3 per cage in an environmentally controlled animal facility maintained at 22°C and 55% relative humidity with a 12-hour light-dark cycle, and fed a semipurified diet, soybean powder being replaced by corn, wheat, bran, and fish meat powders to minimize isoflavone contamination (Oriental Yeast Co Ltd, Tokyo, Japan). On day 50 after birth, they were injected intravenously with MNU (Sigma-Aldrich Japan, Tokyo), 50 mg/kg body weight, then euthanized by bleeding from the inferior vena cava under anesthesia at days 5, 10, 15, 20, 25, or 56 thereafter.

For the study of sensitivity for detection of early lesions (5–25 days after MNU), incidences of proliferative intraductal lesions (PIL) in whole mount preparations from the right abdominal-inguinal mammary glands (AIMG) and 2 histologic sections prepared from proximal and distal halves of the left AIMG of the same animals were compared. For assessment of chemopreventive effects, animals were fed basal diet containing 0.25% (w/w) of soybean isoflavones (provided by Kikkoman Corporation, Japan) and were sacrificed on days 20 and 56 for the comparison of data on proliferative lesion development using whole mounts and histologic sections. The isoflavone mix cantained daidzein (38.32%), genistein (30.14%), glycitein (5.07%) (total, 73.53%), with some saponin, soybean pectin, and amino acids as other components. Tumor weight was measured by weighing excised grossly visible nodular lesions at necropsy. The experiments were conducted according to the "Guidelines for Animal Experiments in National Cancer Center" of the Committee for Ethics of Animal Experimentation of the National Cancer Center, Japan.

Whole Mount Mammary Gland Preparations

Whole mounts were carefully made by removing the mammary fat pad including the right side AIMG (Figure 1), then fixed in 10% buffered formalin for 12–18 hours after stretching on filter papers, rinsed in distilled water for 1 hour,

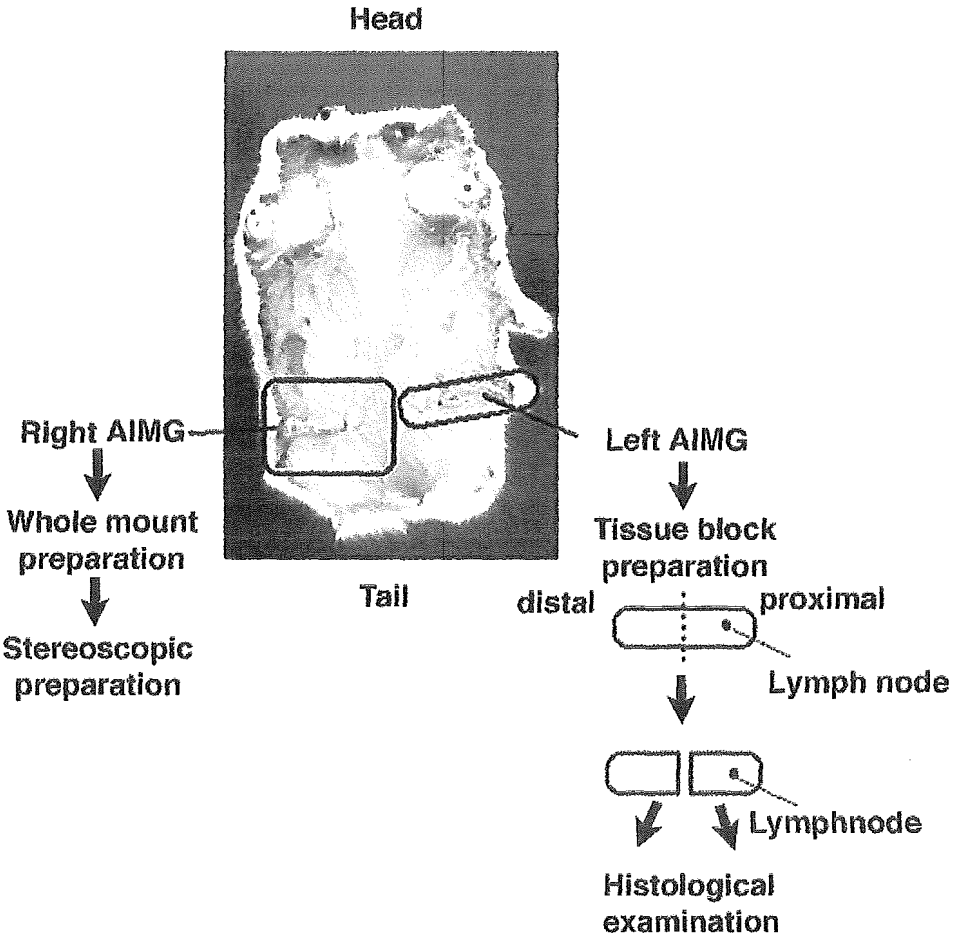

FIGURE 1.—Method for preparation of whole mount preparations and tissue block paraffin sections from AIMG. Whole mounts were taken from the right AIMG and tissue blocks were from the left side. The tissue blocks were excised with fat pad then cut into 2 pieces, processed for paraffin embedding then sectioned in the proximal to distal axis.

immersed overnight in alum carmine, then rinsed again in distilled water. After the staining was completed, the whole mounts were dehydrated through a series of ethanols (70, 95, and 100%), diethyl ether, and cleared in benzene. Each whole mount was then placed in a clear heat seal pouch filled with cedar oil (Wako Pure Chemical, Osaka, Japan). PIL were viewed under a low-power stereoscopic microscope. Some PIL and mammary ducts on days 15 and 20 were subjected to histological analysis after direct excision under a stereoscope and routine processing for paraffin embedding.

Histological Examination

For the histological examination of the left side AIMG, mammary tissues were excised from the subcutaneous tissue with scissors along with the fat pads, then cut into 2 pieces, the proximal region including a lymph node and the distal region. After fixation in acetone, they were separately embedded in paraffin, and 4-μm thick sections for each block, a total of 2 sections along the longitudinal axis from the proximal to the distal regions, were prepared and stained with HE (Figure 1). This simple method was utilized for histological examination of the mammary glands on days 5–25. On day 56, tumors were individually excised and subjected to histological examination. Lesions were classified based on the criteria described by Russo (22) and Singh (26). Small epithelial proliferative lesions without invasion were classified as intraductal proliferations and atypical hyperplasias, the latter showing slight cellular and structural atypia. Cases with obvious invasion were diagnosed as adenocarcinomas. Atypical hyperplasias and adenocarcinomas were combined as early carcinomas when assessing effects of soy isoflavones on day 20 since differential diagnosis between atypical hyperplasias and small adenocarcinomas was often difficult and unnecessary for the purpose of the study. Lesion multiplicity was calculated by dividing the number of total lesions by the areas of sections and expressed as number per cm^2. Acetone fixation is routinely used in our laboratory because of better conservation of antigenicity than with formalin as reported previously (6, 23).

Statistics

The data for tumor incidences were analyzed by the Fisher's exact probability test. Differences in quantitative values for lesion multiplicity were assessed with Dunnett's t-test.

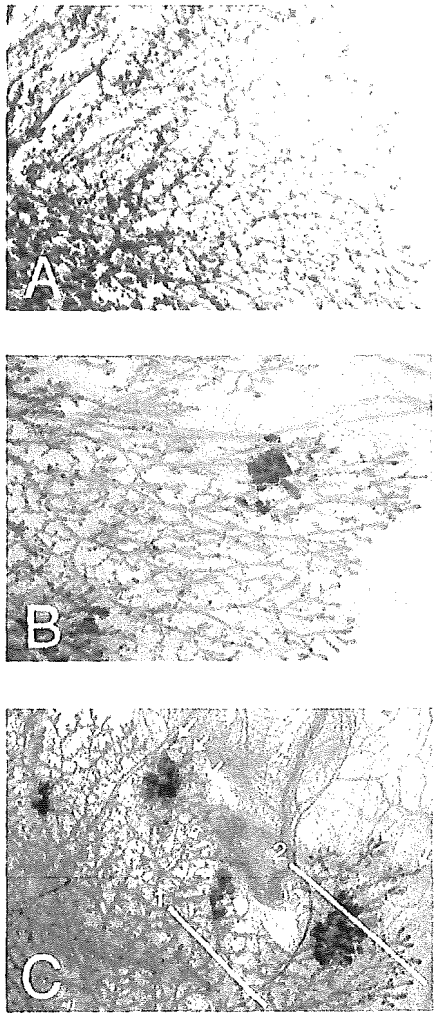

FIGURE 2.—Representative whole mount preparations of AIMG at 0 (A), 15 (B), and 20 (C) days after treatment with MNU, showing the gross appearance of mammary glands. The whole mounts were stained with alum carmine as described in the Materials and Methods section. Arrows indicate TEB and the dark nodular foci are PIL. Lines 1 and 2 indicate the planes from which histological sections were prepared for Figure 3.

RESULTS

Since establishment of a short term, simple method for assessing mammary chemical carcinogenesis was our prime objective, AIMG only were subjected to preparation of whole mounts and histologic sections, unless otherwise specified. In whole mounts, no gross lesions were detected until day 10 (Figure 2A). Typical PIL were firstly observed on day 15 in Hras128 rats (Figure 2B). At day 20 and thereafter, all the rats had such lesions, as shown in Figure 2C. Most PIL (dark irregular shaped masses) were found located proximal to terminal endbuds (TEBs) (arrows in Figures 2B and 2C) considered as targets of chemical carcinogens in the mammary glands (20). Histological analysis of whole mount preparations indicated that the PIL were intraductal proliferations (Figure 3A), atypical hyperplasias (Figure 3B), and adenocarcinomas (Figures 3C and 3D), clearly correlating with the histological appearance of lesions in tissue block preparations of the contralateral AIMG. Therefore, for the assessment of tumor incidence and multiplicity, 2 slices from each block taken from AIMG were subjected to time sequence histological analysis (Figure 1, right half).

Although no lesions could be detected in whole mount preparations on day 10, intraductal proliferations were found in histologic sections. At day 15, both foci of intraductal proliferation and atypical hyperplasias were detected. On day 20, in addition to high incidences of intraductal proliferations and atypical hyperplasias, adenocarcinomas were observed. Incidences of PIL in whole mounts and lesions in the histologic sections reached 100% by day 25, and that

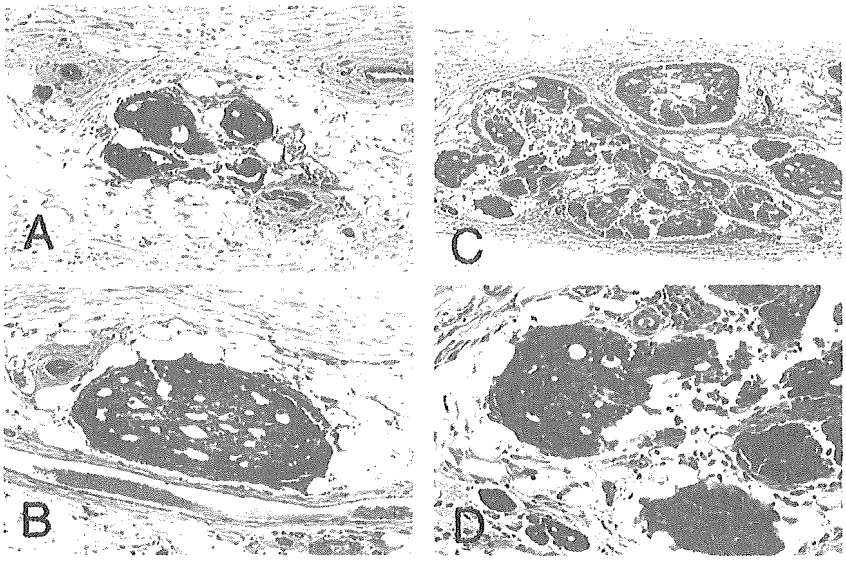

FIGURE 3.—Histological appearance of lesions in sections sequentially prepared from a whole mount preparation. An intraductal proliferation (A) observed in the section from plane 1, and an atypical hyperplasia (B) and adenocarcinomas (C, D) from plane 2 in Figure 2C, respectively. The magnifications of photomicrographs are ×50 in A–C and ×70 for D.

of palpable adenocarcinomas in Hras128 rats did by day 56 (Table 1). Incidences of the tumors in right and left sides of entire mammary glands were the same on day 56.

Data for suppressive effects of soy isoflavones on mammary tumor incidence and multiplicity data between whole mounts and tissue block section of rats sacrificed on day 20 are summarized in Table 2. With whole mounts, the numbers of PIL/rat in isoflavone fed rats were significantly decreased compared to the basal diet group. Similarly, in the tissue block sections, the incidence and number of malignant lesions (atypical hyperplasias and adenocarcinomas) in the isoflavone fed group were significantly lower than in the basal diet group (Table 2). Although there was no difference in tumor incidence between the 2 groups on day 56, the mean tumor weight in the transgenic rats fed isoflavones was approximately one fourth of that in the basal diet group. Only one out of 12 nontransgenic rats fed basal diet developed an adenocarcinoma on day 56, and no statistically significant effect of isoflavones could be detected (Table 3).

DISCUSSION

The present study showed that a simple method with examination of only 2 histologic sections through AIMG is sensitive and more practical for early detection of small neoplastic lesions than examination of whole mount preparations of the contralateral glands. Furthermore, we obtained clear evidence that the same approach is appropriate for assessment of isoflavone inhibition.

Whole mount preparations are frequently used as a convenient method for the examination of small proliferative lesions in entire mammary glands without excising each gland (13, 33). However, since the whole mount preparation requires considerable time and effort to remove the mammary tissue and an assay model requires a certain number of animals for the purpose of effective statistical analyses, it is not practically suitable for evaluation of effects of carcinogens and modifying compounds. The present comparison of sensitivity and practicability for detection of small early lesions indicated that examination of only 2 histologic sections

TABLE 1.—Incidences (%) of proliferative intraductal lesions (PIL) in the abdominal–inguinal mammary glands (AIMG).

			Whole mounts	Histological examination of tissue blocks			
Genotype	Days after MNU	Number of rats	PIL[a]	Intraductal proliferation	Atypical hyperplasia	Adenocarcinoma	Total
Tg	5	9	0 (0)	0 (0)	0 (0)	0 (0)	0 (0)
	10	9	0 (0)	4 (44)	0 (0)	0 (0)	4 (44)
	15	9	4 (44)	8 (89)	4 (44)	0 (0)	8 (89)
	20	11	11 (100)	11 (100)	9 (82)	5 (45)	11 (100)
	25	9	9 (100)	9 (100)	9 (100)	9 (100)	9 (100)
	56[b]	9	—	9 (100)	9 (100)	9 (100)	9 (100)
Non-Tg	25	9	0 (0)	0 (0)	0 (0)	0 (0)	0 (0)

[a]Proliferative intraductal lesions.
[b]Multiple carcinoma development occupying the entire regional mammary glands.
—Not prepared due to technical difficulties.

TABLE 2.—Suppressive effects of soy isoflavones on mammary carcinogenesis as assessed by whole mounts and histological preparations of AIMG on day 20 after MNU injection.

Treatment	Number of rats	Whole mounts[a] Number of PIL/rat (mean ± SD)	Early carcinomas[b] in tissue blocks Incidence (%)	No./cm²
Isoflavones	5	26.4 ± 13.4[c]	2(40)[c]	0.50 ± 0.86[c]
Basal diet	4	47.0 ± 10.7	4(100)	3.89 ± 3.51

[a]PIL, proliferative intraductal lesions in whole mounts.
[b]Including atypical hyperplasia.
[c]$p < 0.05$ as compared to basal diet group.

is sensitive and more practical than employment of whole mount preparations. Although examination of all mammary glands may increase the sensitivity of detection, it is of great advantage that as few as 2 histologic sections can be used without great loss of accuracy (Table 1). Our assay system has the distinct advantage of requiring only a short experimental period, which might allow reduction in the number of animals required if many compounds need be evaluated.

Hras128 rats develop palpable adenocarcinomas as early as 20 days after MNU administration at an incidence of about 45%. The latency is in good agreement with the 21 days observed when MNU (50 mg/kg) was administered i.p. to 21-day-old weaning rats (34) (Table 2). We therefore speculate that the mammary gland of the 50-day-old Hras128 rat biologically resembles that of young immature wild-type animals (32, 33). In fact the number of TEBs in 49-day-old Hras128 rats is greater than that in their wild-type counterparts (Y. Matsuoka, unpublished data). It should be noted that PIL in whole mounts in the current study were located proximal to TEB (Figures 1B and 1C), the distance from the tips of TEB perhaps representing the time lag during which TEBs migrate to sites distal to those where the initial carcinogenic events occur.

The data shown in Table 1 provide a number of insights about the sequence of occurrence of morphologically detectable changes during chemically induced mammary carcinogenesis in Hras128 rats. No morphologically detectable lesions were apparent over the first 5 days following carcinogenic insult. At some point between day 5 and 10 after MNU injection, intraductal proliferation occurred in 44% of the animals. The subsequent emergence of both atypical hyperplasias and adenocarcinomas at day 20 is consistent with the hypothesis that foci of intraductal proliferation evolve through atypical hyperplasia to become invasive carcinomas. However, it is also possible that some foci progress directly to adenocarcinomas without an atypical hyperplasia stage, as proposed by other investigators from studies of non-transgenic rats (21, 34). Furthermore, our results indicate that carcinogenic process in Hras128 rats is fundamentally the same as observed in nontransgenic rats, albeit with an extremely short latent period.

Soy isoflavones (eg, genistein) are widely considered to be responsible for the low rate of breast cancer in Asian women and several possible mechanisms have been proposed. These include inhibition of topoisomerase II and protein tyrosine kinase activity, induction of differentiation and apoptosis, and suppression of angiogenesis and invasion (4, 5, 8, 9, 24, 25). Our findings of significant reduction in numbers of PIL and more remarkably of atypical hyperplasias in AIMG of animals given soy isoflavones at day 20 is thus in line with the literature (Table 2). Similarly, mammary carcinomas as assayed by total weights for each rat also showed a clear decrease (Table 3). Although a rapid induction model has been reported in which preneoplastic proliferative lesions and carcinomas could be induced 21 days after MNU injection in immature animals (33, 34), treatment before weaning is not practical, especially to assess effects of dietary compounds. Furthermore, that our transgenic rats are sexually mature may be advantageous with regard to practical application of the assay models for the search of chemopreventive agents.

Since all of the transgenic rats develop mammary carcinomas within a month after MNU administration, our animals have potential for use in a short-term screening system for preventive agents of mammary carcinogenesis such as isoflavones. Further modification by replacing MNU for DMBA or other carcinogens allowing simple oral administration warrants further practical exploration (11).

TABLE 3.—Suppressive effects of soy isoflavones as assessed by tissue block histological examination on AIMG on day 56 after MNU injection.

Genotype	Treatment	Number of rats	Number of rats with lesions[a] (%)	Tumor weight[a] (g)/rat (mean ± SD)
Tg	Isoflavones	11	11 (100)	7.7 ± 5.9[b]
	Basal diet	10	10 (100)	28.9 ± 17.3
Non-Tg	Isoflavones	11	0 (0)	0
	Basal diet	12	1 (8)	0.1

[a]Grossly visible nodular lesions at autopsy, diagnosed as mostly adenocarcinomas.
[b]$p < 0.01$ as compared to basal diet group.

ACKNOWLEDGMENTS

This work was supported in part by A Grant-in-Aid for Scientific Research on Priority Areas (KAKENHI) from the Ministry of Education, Science, Sports, and Culture of Japan, a Grant-in-aid for the Second Term Comprehensive 10-Year Strategy for Cancer Control, a Grant-in-aid for Cancer Research from the Ministry of Health, Labour, and Welfare of Japan, and a Grant-in Aid for The Long-range Research Initiative from the Japan Chemical Industry Association (CC05-01). T. Hamaguchi and K. Fukamachi are recipients of Research Resident Fellowships from the Foundation of Promotion Cancer Research, supported by the Second Term Comprehensive 10-Year Strategy for Cancer Control. We are grateful to Dr. S. Fukushima of Osaka City University for suggestions and encouragement, to Dr. Malcolm Moore for critical reading of the manuscript, and to Dr. Obata, Kikkoman Corporation for generous provision of soy isoflavones. We also thank Ms. A. Yamaguchi for technical and Ms. A. Ichikawa for secretarial assistance.

REFERENCES

1. Ando K, Saitoh A, Hino O, Takahashi R, Kimura M, Katsuki M (1992). Chemically induced forestomach papillomas in transgenic mice carry mutant human c-Ha-ras transgenes. *Cancer Res* 52: 978–982.
2. Asamoto M, Ochiya T, Toriyama-Baba H, Ota T, Sekiya T, Terada M, Tsuda H (2000). Transgenic rats carrying human c-Ha-ras proto-oncogenes are highly susceptible to *N*-methyl-*N*-nitrosourea mammary carcinogenesis. *Carcinogenesis* 21: 243–249.

3. Asamoto M, Toriyama-Baba H, Ohnishi T, Naito A, Ota T, Ando A, Ochiya T, Tsuda H (2002). Transgenic rats carrying human c-Ha-ras proto-oncogene are highly susceptible to *N*-Nitrosomethylbenzylamine induction of esophageal tumorigenesis. *Jpn J Cancer Res* 93: 744–751.
4. Barnes S, Peterson TG (1995). Biochemical targets of the isoflavone genistein in tumor cell lines. *Proc Soc Exp Biol Med* 208: 103–108.
5. Constantinou A, Huberman E (1995). Genistein as an inducer of tumor cell differentiation: possible mechanisms of action. *Proc Soc Exp Biol Med* 208: 109–115.
6. de Camargo JL, Tsuda H, Asamoto M, Tagawa Y, Wada S, Nagase S, Ito N (1993). Modifying effects of chemicals on the development of liver preneoplastic placental glutathione *S*-transferase positive foci in analbuminemic and Sprague-Dawley rats. *Toxicol Pathol* 21: 409–416.
7. Dragan Y, Valdes R, Gomez-Angelats M, Felipe A, Javier Casado F, Pitot H, Pastor-Anglada M (2000). Selective loss of nucleoside carrier expression in rat hepatocarcinomas. *Hepatology* 32: 239–246.
8. Fotsis T, Pepper M, Adlercreutz H, Fleischmann G, Hase T, Montesano R, Schweigerer L (1993). Genistein, a dietary-derived inhibitor of in vitro angiogenesis. *Proc Natl Acad Sci USA* 90: 2690–2694.
9. Fotsis T, Pepper MS, Aktas E, Breit S, Rasku S, Adlercreutz H, Wahala K, Montesano R, Schweigerer L (1997). Flavonoids, dietary-derived inhibitors of cell proliferation and in vitro angiogenesis. *Cancer Res* 57: 2916–2921.
10. French J, Storer RD, Donehower LA (2001). The nature of the heterozygous Trp53 knockout model for identification of mutagenic carcinogens. *Toxicol Pathol* 29(Suppl): 24–29.
11. Han BS, Fukamachi K, Takasuka N, Ohnishi T, Maeda M, Yamasaki T, Tsuda H (2002). Inhibitory effects of 17-beta-estradiol and 4-*n*-octylphenol on 7,12-dimethylbenz[a]anthracene-induced mammary tumor development in human c-Ha-ras proto-oncogene transgenic rats. *Carcinogenesis* 23: 1209–1215.
12. Hully JR, Su Y, Lohse JK, Griep AE, Sattler CA, Haas MJ, Dragan Y, Peterson J, Neveu M, Pitot HC (1994). Transgenic hepatocarcinogenesis in the rat. *Am J Pathol* 145: 386–397.
13. Lamartiniere CA, Moore J, Holland M, Barnes S (1995). Neonatal genistein chemoprevents mammary cancer. *Proc Soc Exp Biol Med* 208: 120–123.
14. Messina MJ, Persky V, Setchell KD, Barnes S (1994). Soy intake and cancer risk: a review of the in vitro and in vivo data. *Nutr Cancer* 21: 113–131.
15. Ota T, Asamoto M, Toriyama-Baba H, Yamamoto F, Matsuoka Y, Ochiya T, Sekiya T, Terada M, Akaza H, Tsuda H (2000). Transgenic rats carrying copies of the human c-Ha-ras proto-oncogene exhibit enhanced susceptibility to *N*-butyl-*N*-(4-hydroxybutyl)nitrosamine bladder carcinogenesis. *Carcinogenesis* 21: 1391–1396.
16. Ozaki K, Sukata T, Yamamoto S, Uwagawa S, Seki T, Kawasaki H, Yoshitake A, Wanibuchi H, Koide A, Mori Y, Fukushima S (1998). High susceptibility of *p53*(+/−) knockout mice in *N*-butyl-*N*-(4-hydroxybutyl)nitrosamine urinary bladder carcinogenesis and lack of frequent mutation in residual allele. *Cancer Res* 58: 3806–3811.
17. Page DL, Dupont WD (1993). Anatomic indicators (histologic and cytologic) of increased breast cancer risk. *Breast Cancer Res Treat* 28: 157–166.
18. Parker SL, Tong T, Bolden S, Wingo PA (1996). Cancer statistics, 1996. *CA Cancer J Clin* 46: 5–27.
19. Russo J, Wilgus G, Russo IH (1979). Susceptibility of the mammary gland to carcinogenesis: I Differentiation of the mammary gland as determinant of tumor incidence and type of lesion. *Am J Pathol* 96: 721–736.
20. Russo J, Russo IH (1987). Biological and molecular bases of mammary carcinogenesis. *Lab Invest* 57: 112–137.
21. Russo J, Gusterson BA, Rogers AE, Russo IH, Wellings SR, van Zwieten MJ (1990). Comparative study of human and rat mammary tumorigenesis. *Lab Invest* 62: 244–278.
22. Russo J, Russo IH (1996). Experimentally induced mammary tumors in rats. *Breast Cancer Res Treat* 39: 7–20.
23. Sato Y, Mukai K, Furuya S, Kameya T, Hirohashi S (1992). The AMeX method: a multipurpose tissue-processing and paraffin-embedding method. Extraction of protein and application to immunoblotting. *Am J Pathol* 140: 775–779.
24. Shao ZM, Alpaugh ML, Fontana JA, Barsky SH (1998). Genistein inhibits proliferation similarly in estrogen receptor-positive and negative human breast carcinoma cell lines characterized by P21WAF1/CIP1 induction, G2/M arrest, and apoptosis. *J Cell Biochem* 69: 44–54.
25. Shao ZM, Wu J, Shen ZZ, Barsky SH (1998). Genistein exerts multiple suppressive effects on human breast carcinoma cells. *Cancer Res* 58: 4851–4857.
26. Singh M, McGinley JN, Thompson HJ (2000). A comparison of the histopathology of premalignant and malignant mammary gland lesions induced in sexually immature rats with those occurring in the human. *Lab Invest* 80: 221–231.
27. Storer RD, Cartwright ME, Cook WO, Soper KA, Nichols, WW (1995). Short-term carcinogenesis bioassay of genotoxic procarcinogens in PIM transgenic mice. *Carcinogenesis* 16: 285–293.
28. Sukumar S, McKenzie K, Chen Y (1995). Animal models for breast cancer. *Mutat Res* 333: 37–44.
29. Tennant RW, Spalding J, French JE (1996). Evaluation of transgenic mouse bioassays for identifying carcinogens and noncarcinogens. *Mutat Res* 365: 119–127.
30. Tennant RW, Stasiewicz S, Mennear J, French JE, Spalding JW (1999). Genetically altered mouse models for identifying carcinogens. *IARC Sci Publ* 123–150.
31. Thompson HJ, Adlakha H (1991). Dose-responsive induction of mammary gland carcinomas by the intraperitoneal injection of 1-methyl-1-nitrosourea. *Cancer Res* 51: 3411–3415.
32. Thompson HJ, Adlakha H, Singh M (1992). Effect of carcinogen dose and age at administration on induction of mammary carcinogenesis by 1-methyl-1-nitrosourea. *Carcinogenesis* 13: 1535–1539.
33. Thompson HJ, McGinley JN, Rothhammer K, Singh M (1995). Rapid induction of mammary intraductal proliferations, ductal carcinoma in situ and carcinomas by the injection of sexually immature female rats with 1-methyl-1-nitrosourea. *Carcinogenesis* 16: 2407–2411.
34. Thompson HJ, McGinley JN, Wolfe P, Singh M, Steele VE, Kelloff GJ (1998). Temporal sequence of mammary intraductal proliferations, ductal carcinomas in situ and adenocarcinomas induced by 1-methyl-1-nitrosourea in rats. *Carcinogenesis* 19: 2181–2185.
35. Thorgeirsson SS, Factor VM, Snyderwine EG (2000). Transgenic mouse models in carcinogenesis research and testing. *Toxicol Lett* 112–113: 553–555.
36. Tsuda H, Asamoto M, Ochiya T, Toriyama-Baba H, Naito A, Ota T, Sekiya T, Terada M (2001). High susceptibility of transgenic rats carrying the human c-Ha-ras proto-oncogene to chemically-induced mammary carcinogenesis. *Mutat Res* 477: 173–182.
37. Yamamoto S, Mitsumori K, Kodama Y, Matsunuma N, Manabe S, Okamiya H, Suzuki H, Fukuda T, Sakamaki Y, Sunaga M, Nomura G, Hioki K, Wakana S, Nomura T, Hayashi Y (1996). Rapid induction of more malignant tumors by various genotoxic carcinogens in transgenic mice harboring a human prototype c-Ha-ras gene than in control non-transgenic mice. *Carcinogenesis* 17: 2455–2461.

American Journal of Pathology, Vol. 168, No. 3, March 2006

DOI: 10.2353/ajpath.2006.050801

Matrix Pathobiology

Discoidin Domain Receptor 1 Contributes to the Survival of Lung Fibroblast in Idiopathic Pulmonary Fibrosis

Wataru Matsuyama, Masaki Watanabe, Yuko Shirahama, Hideo Mitsuyama, Ikkou Higashimoto, Mitsuhiro Osame, and Kimiyoshi Arimura

From the Division of Respiratory Medicine, Respiratory and Stress Care Center, Kagoshima University Hospital, Kagoshima, Japan

Idiopathic pulmonary fibrosis (IPF), characterized by fibroblast proliferation and accumulation of extracellular matrix, including collagen, is a chronic progressive disorder that results in lung remodeling and fibrosis. However, the cellular mechanisms that may make fibroblasts resistant to apoptosis have not been completely elucidated. Discoidin domain receptor 1 (DDR1), a receptor tyrosine kinase whose ligand is collagen, is expressed *in vivo* and contributes *in vitro* to leukocyte differentiation and nuclear factor (NF)-κB activation, which may play an important role in fibroblast survival. In this study, we examined *in vivo* and *in vitro* DDR1 expression and its role in cell survival using fibroblasts obtained from IPF and non-IPF patients. Immunohistochemically, fibroblasts present in fibroblastic foci expressed endogenous DDR1. The DDR1 expression level was significantly higher in fibroblasts from IPF patients, and the predominant isoform was DDR1b. In IPF patients, DDR1 activation in fibroblasts inhibited Fas ligand-induced apoptosis and resulted in NF-κB nuclear translocation. Suppression of DDR1 expression in fibroblasts by siRNA abolished these effects, and an NF-κB inhibitor abrogated the anti-apoptotic effect of DDR1 activation. We propose that DDR1 contributes to fibroblast survival in the tissue microenvironment of IPF and that DDR1 up-regulation may occur in other fibroproliferative lung diseases as well. *(Am J Pathol 2006, 168:866–877; DOI: 10.2353/ajpath.2006.050801)*

Idiopathic pulmonary fibrosis (IPF) is a progressive and usually fatal pulmonary disorder that is characterized by fibroblast proliferation and abnormal accumulation of extracellular matrix (ECM) molecules, particularly fibrillar collagens.[1] An important feature of IPF is the presence of fibroblast foci, which are widely distributed throughout the lung parenchyma.[1] The fibroblastic foci represent microscopic zones of acute lung injury (ALI) in which fibroblasts migrate, proliferate, and contribute to the accumulation of ECM molecules in the damaged alveolus. Subsequently, abnormal remodeling of the lung architecture results from interstitial and intraluminal deposition of connective tissue.[2] In these processes, the release of fibrogenic cytokines may result in fibroblast proliferation and migration to various sites in the lung, followed by differentiation of the fibroblast phenotype.[3,4] This differentiation of fibroblasts is considered key to the chronic nature of IPF, and several reports suggest that fibroblasts in IPF appear to be more resistant to apoptosis,[5,6] a process that is important in both the pathogenesis and resolution of pulmonary fibrotic lesions.[7] However, the cellular mechanisms specifically involved in fibroblast apoptosis have not been completely elucidated. Furthermore, the assumption that fibroblasts in IPF are more resistant to apoptosis remains controversial to date.

Discoidin domain receptor 1 (DDR1) is a receptor tyrosine kinase that is activated by binding with its ligand, collagen.[8,9] DDR1 has a unique extracellular domain that is homologous to discoidin 1 of *Dictyostelium discoideum*.[10] DDR1 is constitutively expressed in normal tissues such as lungs, kidneys, colon, and brain; in tumor cells of epithelial origins, such as those from mammary, ovarian, and lung carcinomas[10]; and also in dermal fibroblasts.[11] Five DDR1 isoforms (a, b, c, d, and e) can be generated by alternative splicing of the *DDR1* gene,[10,12] and two of these isoforms (1a and 1b) have known func-

Supported by the Japan Society for the Promotion of Science (grant-in-aid for scientific research no. 16790447), The Sumitomo Foundation (grant no. 040010), the Nagao Memorial Fund, the Uehara Memorial Foundation, and the Kanae Foundation for Life and Socio-Medical Science.

Accepted for publication October 28, 2005.

Address reprint requests to Wataru Matsuyama, Division of Respiratory Medicine, Respiratory and Stress Care Center, Kagoshima University Hospital, Sakuragaoka 8-35-1, Kagoshima 890-8520, Japan. E-mail: vega@xa2.so-net.ne.jp.

tions.[13,14] The DDR1a and DDR1b isoforms differ from each other by an in-frame insertion of 111 bp that codes for an additional 37-amino acid peptide in the proline-rich juxtamembrane region. The 37-amino acid insertion in DDR1b contains the LXNPXY motif that corresponds to the consensus-binding motif of the Shc phosphotyrosine-binding domain.[10] Disruption of the *DDR1* gene in mice resulted in viable animals that were significantly smaller in size than their littermates, whereas female DDR1-null mice showed defects in blastocyst implantation and mammary gland development.[15] These previous observations indicate that DDR1 contributes to tissue development. In addition, we recently found that DDR1b activation can induce leukocyte differentiation[16] and activate transcriptional factor nuclear factor (NF)-κB,[17] which is reported to play an important role in fibroblast survival.[18]

In this study, we obtained primary cultures of fibroblasts from IPF patients and non-IPF patients and examined the DDR1 expression. We observed that fibroblasts obtained from IPF patients predominantly expressed DDR1b and DDR1 activation on IPF fibroblasts inhibited Fas ligand (FasL)-induced apoptosis.

Materials and Methods

This study was reviewed and approved by the Kagoshima University Faculty of Medicine Committee on Human Research.

Immunohistochemistry

Biopsied lung tissues obtained from three IPF patients and three non-IPF patients were examined for the presence of DDR1 by immunohistochemical staining using rabbit anti-DDR1 antibodies (Santa Cruz Biotechnology, Santa Cruz, CA) and visualized by the diaminobenzidine method, as described previously.[19] Briefly, 4-μm-thick sections were mounted on poly-L-lysine-coated slides, dewaxed, and washed in Tris-buffered saline (pH 7.4) for 10 minutes. For optimal antigen retrieval, the sections were pressure cooked in 0.01 mol/L citrate buffer (pH 6.0) for 90 seconds. Endogenous peroxidase activity was blocked using a 3% hydrogen peroxide solution in methanol for 10 minutes. After two washes in phosphate-buffered saline (PBS) containing 1% saponin, the blocking reaction was performed as reported previously.[20] The sections were incubated with a 1:50 dilution of the primary antibody solution for 2 hours at room temperature. Negative control slides were incubated with rabbit IgG (R&D Systems, Minneapolis, MN). Secondary biotinylated anti-immunoglobulin antibodies (R&D Systems) were added, and the mixture was incubated for 30 minutes at room temperature. After washing, the sections were incubated with streptavidin conjugated to horseradish peroxidase (Amersham, Arlington Heights, IL) and then rinsed with deionized water. Diaminobenzidine substrate solution was added, and the mixture was incubated for 10 minutes. A positive result was indicated by a brown color reaction.

Patients with Lung Fibrosis

Fibroblasts were derived from lung tissue samples obtained from seven IPF patients. The lung tissue samples were obtained by video-assisted lung biopsy for diagnosis. IPF was diagnosed in accordance with the American Thoracic Society/European Respiratory Society consensus criteria,[21,22] including the characteristic morphology of usual interstitial pneumonia. The average age of the seven patients (six men and one woman) was 59.5 years (range, 47 to 68 years). Of the seven patients, six were ex-smokers and one was a nonsmoker. None of the patients were treated with immunosuppressive drugs, including corticosteroids.

Non-IPF Patients

Fibroblasts were derived from lung tissue samples obtained from six patients (four men and two women) undergoing lung surgery for the removal of a primary lung tumor. Normal lung tissue from a noninvolved segment, at a distance from the solitary lesion, was obtained. The average age of the six patients was 62.4 years (range, 41 to 70 years); two patients were nonsmokers and four were ex-smokers.

Acute Lung Injury (ALI) Patients

Fibroblasts were also derived from lung samples obtained from four patients who suffered from adult respiratory distress syndrome (two biopsy samples and two autopsy samples). The average age of the four patients was 52.3 years (range, 31 to 61 years). All of the patients were nonsmokers.

Culture of Fibroblasts

Human lung fibroblasts were cultured from lung explants according to the method described by Akamine and colleagues.[23] The fibroblasts were cultured in Dulbecco's modified Eagle's medium containing 10% fetal calf serum supplemented with 100 U/ml penicillin and 100 g/ml streptomycin (complete medium). The cells were used at passage 5. All of the cell cultures were immunohistochemically evaluated at passage 5. Essentially, 100% of the cells were fibroblasts as indicated by the strong labeling with anti-prolyl-4-hydroxylase, anti-vimentin, and anti-CD90 monoclonal antibodies (PharMingen, San Diego, CA).[24] Staining with anti-smooth muscle myosin heavy chain-1, anti-cytokeratin, and anti-CD31 antibodies (PharMingen) was always negative, indicating that the cultures did not contain smooth muscle cells or epithelial or endothelial cells.

Flow Cytometry Analysis

To detect DDR1 and α-smooth muscle actin (α-SMA) expression on fibroblasts, 5×10^5 cells were collected after five passages. The cells were washed three times with PBS and then incubated with human serum (pooled

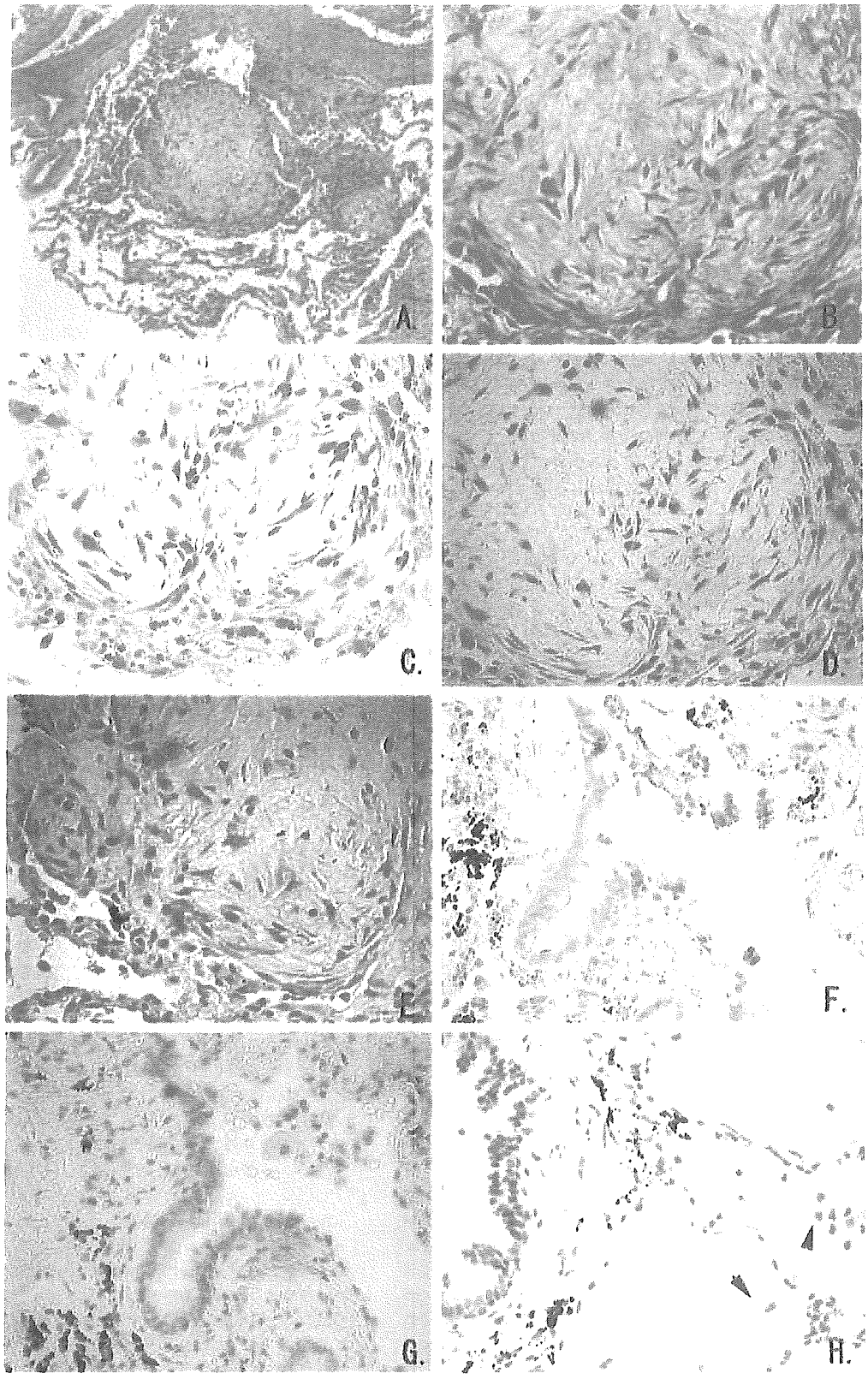

Figure 1. Immunohistochemistry of the biopsied lung of an IPF patient. **C:** Fibroblasts in the fibroblastic foci show strong positive staining for DDR1. **C** and **E:** Inflammatory cells in the IPF lesion are also stained positive for DDR1. **E:** The bronchoepithelial cells are negative for DDR1. In the non-IPF lung, only alveolar macrophages are stained weakly positive for DDR1 (**arrowheads**). **A** and **B:** *H&E staining*; **D** and **G:** *nonspecific rabbit IgG*; **E:** *negative control* for second antibody. Original magnifications: ×300 (**A**); ×500 (**B–H**).